

Journal of Visualized Experiments

Visualizing Solution Structure at Solid-Liquid Interfaces Using Three-Dimensional Fast Force Mapping --Manuscript Draft--

Article Type:	Invited Methods Article - JoVE Produced Video
Manuscript Number:	JoVE62585R2
Full Title:	Visualizing Solution Structure at Solid-Liquid Interfaces Using Three-Dimensional Fast Force Mapping
Corresponding Author:	Elias Nakouzi Pacific Northwest National Laboratory Richland, Washington UNITED STATES
Corresponding Author's Institution:	Pacific Northwest National Laboratory
Corresponding Author E-Mail:	elias.nakouzi@pnnl.gov
Order of Authors:	Elias Nakouzi Sakshi Yadav Benjamin Legg Shuai Zhang Jinhui Tao Christopher Mundy Gregory Schenter Jaehun Chun James De Yoreo
Additional Information:	
Question	Response
Please indicate whether this article will be Standard Access or Open Access.	Standard Access (US\$2,400)
Please specify the section of the submitted manuscript.	Chemistry
Please indicate the city, state/province, and country where this article will be filmed . Please do not use abbreviations.	Richland, WA
Please confirm that you have read and agree to the terms and conditions of the author license agreement that applies below:	I agree to the Author License Agreement
Please provide any comments to the journal here.	Thanks
Please indicate whether this article will be Standard Access or Open Access.	Standard Access (\$1400)

TITLE:

Visualizing Solution Structure at Solid-Liquid Interfaces Using Three-Dimensional Fast Force Mapping

AUTHORS AND AFFILIATIONS:

Elias Nakouzi,^{1*} Sakshi Yadav,¹ Benjamin A. Legg,¹ Shuai Zhang,^{1,2} Jinhui Tao,¹ Christopher J. Mundy,^{1,3} Gregory K. Schenter,^{1,4} Jaehun Chun,^{1,5} James J. De Yoreo^{*1,2}

¹Physical and Computational Sciences Directorate, Pacific Northwest National Laboratory, Richland, Washington, United States

²Department of Materials Science and Engineering, University of Washington, Seattle, Washington, United States

³Department of Chemical Engineering, University of Washington, Seattle, Washington, United States

⁴Department of Chemistry, Washington State University, Pullman, Washington, United States

⁵CUNY City College of New York, New York, United States

Email addresses:

Elias Nakouzi (elias.nakouzi@pnnl.gov)

Sakshi Yadav (sakshi.yadav@pnnl.gov)

Benjamin A. Legg (benjamin.legg@pnnl.gov)

Shuai Zhang (zhangs71@uw.edu)

Jinhui Tao (jinhui.tao@pnnl.gov)

Christopher J. Mundy (chris.mundy@pnnl.gov)

Gregory K. Schenter (greg.schenter@pnnl.gov)

Jaehun Chun (jaehun.chun@pnnl.gov)

James J. De Yoreo (james.deyoreo@pnnl.gov)

*Corresponding Authors:

Elias Nakouzi (elias.nakouzi@pnnl.gov)

James J. De Yoreo (james.deyoreo@pnnl.gov)

SUMMARY:

Here, we present a protocol for using three-dimensional fast force mapping – an atomic force microscopy technique – for visualizing solution structure at solid-liquid interfaces with the subnanometer resolution by mapping the tip-sample interactions within the interfacial region.

ABSTRACT:

Amongst the challenges for a variety of research fields are the visualization of solid-liquid interfaces and understanding how they are affected by the solution conditions such as ion concentrations, pH, ligands, and trace additives, as well as the underlying crystallography and chemistry. In this context, three-dimensional fast force mapping (3D FFM) has emerged as a promising tool for investigating solution structure at interfaces. This capability is based on atomic force microscopy (AFM) and allows the direct visualization of interfacial regions in three spatial

dimensions with sub-nanometer resolution. Here we provide a detailed description of the experimental protocol for acquiring 3D FFM data. The main considerations for optimizing the operating parameters depending on the sample and application are discussed. Moreover, the basic methods for data processing and analysis are discussed, including the transformation of the measured instrument observables into tip-sample force maps that can be linked to the local solution structure. Finally, we shed light on some of the outstanding questions related to 3D FFM data interpretation and how this technique can become a central tool in the repertoire of surface science.

INTRODUCTION:

Many interesting phenomena occur within a few nanometers of a solid-liquid interface where classical theories for colloidal interactions break down¹. Solvent molecules and ions organize into unexpected patterns² and diverse processes, such as catalysis³, ion adsorption^{4,5}, electron transfer^{6,7}, bio-molecular assembly⁸, particle aggregation⁹, attachment^{10,11}, and assembly^{12,13}, can occur. However, few techniques can characterize the solution structure at the interface, particularly with sub-nanometer 3D resolution. In this context, three-dimensional fast force mapping (3D FFM)—a technique based on atomic force microscopy (AFM)—has emerged as a useful tool for determining interfacial solution structure^{14,15} and understanding its impact on such phenomena.

In general, AFM techniques employ a cantilever with a nanosized tip to characterize surfaces using two main classes of measurements: topographic imaging that measures the height of a substrate at every xy pixel or force measurements that quantify mechanical properties, colloidal interactions^{16,17}, or adhesive forces between a functionalized tip and the substrate. Today, the capabilities of this versatile instrument extend far beyond these traditional applications; skilled users operating modern instruments can measure electrical, magnetic, and chemical surface properties by coupling force microscopy to spectroscopy and other methods¹⁸. Perhaps the most fascinating advances have been the ability to image materials and processes in their native solutions, with nanoscale spatial resolution, in real time¹⁹⁻²¹. This latter capability facilitated the development of 3D FFM, which extends AFM measurements into the third spatial dimension by combining 1D force curves with topographic imaging¹⁴. Specifically, the tip acquires consecutive force curves at each xy coordinate to produce a 3D map of the forces detected by the tip at the solid-liquid interface. The novelty here is that a sufficiently fast and sensitive tip can detect minor force gradients corresponding to the local distribution of molecules to map the interfacial solution structure.

To date, 3D FFM has been developed by only a few research groups, which, in our opinion, is not due to its technical limitations but rather the need for customizing instruments in-house to perform these measurements. However, 3D FFM was recently commercialized and is now accessible to researchers of all relevant disciplines. From a scientific point of view, this technique has a broad and multi-disciplinary appeal. For example, the first 3D FFM experiments were performed on mineral-solution systems^{15,22-24}, where important questions included understanding mechanisms of crystal growth and dissolution, the adsorption of ions and molecules, and the role of hydration layers in particle aggregation and attachment. Successful

experiments have identified calcium and magnesium atoms in a dolomite crystal lattice²⁵, visualized solution structure around calcite point defects²⁶, and imaged ion adsorption at mica^{27,28} and fluorite^{24,29} surfaces.

Beyond visualizing mineral-solution interfaces, 3D FFM can provide insights into fundamental questions in surface and colloidal physics, such as the scaling of short-range colloidal interactions, the structure of electric double layers at a molecular level, and the nature and origins of solvation forces. These measurements have important implications for electrochemistry and battery research, as 3D FFM can map electrode-electrolyte interfaces and probe their response to electric fields³. Other applications in materials science include understanding phenomena that occur at the surfaces of separation membranes, heterogeneous catalysts, and polymer coatings. As this capability develops further, we anticipate that it will also play an important role in imaging biomolecules and delineating the role of interactions, ions, and solvent molecules in their self-assembly.

One of the key aspects for advancing data interpretation in 3D FFM is benchmarking against other experimental and simulation tools that have been previously used to study solid-liquid interfaces. For example, techniques based on X-ray reflectivity or diffraction measure electron density profiles that can be mapped to the distribution of ions and solvent molecules as a function of height from the interface³⁰⁻³³. This approach has been successful for a range of mineral-solution systems but remains limited to large atomically smooth surfaces and is often incapable of producing laterally resolved data. Other techniques, such as sum frequency generation spectroscopy, provide evidence of particular aspects of solvent structuring at mineral surfaces, such as the orientation of solvent molecules at the surface, but not direct visualization of the structure^{34,35}. Moreover, molecular dynamics simulations have advanced significantly and can now routinely probe solvent distribution profiles at crystal surfaces^{4,36-39}. While each of these techniques has its own challenges and limitations, they form a complementary suite of tools for investigating interfacial solution structure; 3D FFM is poised to contribute significantly to this regard and expand the range of solid-liquid systems that can be studied, as well as the research questions that can be answered.

A pre-requisite for implementing 3D FFM on a particular sample, is the ability to obtain topographic images with the desired spatial resolution. For a detailed experimental protocol on high-resolution AFM imaging, the reader is referred to a recent manuscript by Miller et al.²⁰. For optimal operation of 3D FFM, it is strongly advised to first master the high-resolution imaging technique described therein. Most of the recommendations in that protocol are applicable and necessary for 3D FFM. In the following protocol, we briefly highlight the main steps for high-resolution imaging but focus on specific considerations for 3D FFM.

PROTOCOL

1. Loading and calibrating the AFM tip

1.1 Clean the cantilever tip by immersing it in water and isopropanol solvents consecutively for several minutes to remove contaminants and organic adsorbates. Other common methods for cleaning include argon-plasma or ultraviolet-ozone surface treatment.

NOTE: Be consistent in the sample and cantilever preparation when comparing different data sets. Changes in the cleaning process might affect the tip properties such as surface chemistry, hydrophilicity, or even shape, and hence influence the measured forces⁴⁰.

1.2 Clean the cantilever holder with water and isopropanol solvents as well.

1.3 Load the cantilever into the holder using the holder clamp or screw, as typical for the AFM instrument in use. Connect the cantilever holder to the AFM.

1.4 Align the laser spot on the tip to maximize the response signal using the AFM software, and then zero the deflection signal.

1.5 Measure the cantilever spring constant in the air. This step is automated on most modern microscopes by recording the thermal fluctuations of the cantilever and fitting the first resonance peak to a simple harmonic oscillator model performed following the manufacturer's protocol.

NOTE: Measuring the spring constant is often overlooked in some AFM applications but is crucial for the correct interpretation of 3D AFM data, particularly for converting data from instrument observables into measured forces, as described in a later section.

2. Loading the substrate and solution

2.1 Disconnect and remove the cantilever holder from the AFM stage and add ~60 μL of the imaging solution onto the cantilever tip. Make sure the tip is fully immersed in the solution. Take care to avoid creating air bubbles during this process.

NOTE: The imaging solution can be anything related to the scientific investigation. As a test solution, use $[\text{KCl}] = 10 \text{ mM}$ or even pure water.

2.2 Cleave the sample (e.g., mica) immediately prior to the measurements to obtain a smooth and clean surface. Rinse the sample with the imaging solution and then add ~100 μL of the same imaging solution onto the sample surface.

2.2.1 Place the cleaned substrate on the sample stage. The substrate size varies depending on the experiment; it could be as large as a $1 \times 1 \text{ cm}^2$ wafer or as small as nanoparticles deposited on a surface.

NOTE: As with any other AFM measurement, having a clean surface is very critical for obtaining reliable 3D data, as the interface is particularly sensitive to contamination by organics and other residues²⁷.

2.3 Return and secure the cantilever holder in its position on the stage. Carefully lower the cantilever position until the solution droplets on the tip, and the sample comes into contact. The sample stage is either controlled by the instrument software or by a physical knob on the instrument body.

2.4 Allow the sample surface to chemically equilibrate and exchange ions with the imaging solution for about 10 min.

2.4.1. As an optional step, remove the cantilever tip, replace the imaging solution with a fresh aliquot, return the cantilever holder, and approach the sample until the tip is again immersed in the solution.

3. Setting instrument parameters for amplitude-modulated AFM measurements

3.1 Acquire another thermal graph while the tip is immersed in the solution. At this point, ensure that the spring constant is fixed at the value calculated in step 1.5, while an instrument parameter (e.g., *AmplnVOLS* parameter) is used to fit the thermal peak. Again, this step is automated on most modern microscopes with a few clicks under the thermal graph section in the instrument software.

NOTE: This parameter calibrates the conversion of the electronic signal detected by the instrument to the tip-sample distance in nanometer values so that the experimentalist can obtain reliable data of the tip position and deflection.

3.2 Tune the cantilever tip by setting the drive frequency (ν_{exc}) at the resonance frequency (ν_e), and subsequently centering the phase shift at 90° close to the resonance frequency. These are instrument parameters that the users can control using the manufacturer's protocol when operating the instrument in the amplitude modulated mode.

NOTE: Some AFM instruments use photothermal excitation, for which the resonance frequency is the same value obtained in step 3.1. This method of tip excitation is highly advantageous for 3D force mapping as it allows a stable imaging conditions, even at very low drive amplitudes.

3.3 Locate the approximate height of the sample surface and carefully approach the tip until it engages with the surface. Do this by changing the setpoint amplitude to approximately ~70% of the free amplitude using the **Set Point** parameter in the instrument software. As the tip approaches the surface, the amplitude drops until it reaches the setpoint value and is thus determined to be engaged at the surface.

3.4 Obtain a single force curve starting at ~200 nm distance from the surface. Typically, this is done in the **Force** panel of the instrument software. Before withdrawing the tip, re-tune and center the phase shift at 90° as in step 3.2. The resonance frequency will decrease slightly due to tip-surface interactions.

NOTE: This step ensures that, during the subsequent 3D FFM measurements, the phase shift is approximately 90 degrees at the retracted tip position.

3.5 Change the set amplitude to ~70% of the free amplitude. Do not use very low setpoint values (large, applied force) as this might pre-maturely damage the tip.

3.6 Acquire a topographic image. For smooth surfaces such as mica, start with a $\sim 20 \times 20 \text{ nm}^2$ image. For rougher surfaces, start by imaging larger areas before quickly locating an atomically smooth $20 \times 20 \text{ nm}^2$ area to image. Carefully examine the acquired images. At this point, the 2D imaging resolution should be at least equivalent to the desired 3D force mapping resolution.

NOTE: Care should be taken to minimize the damage incurred by the tip. For example, do not take more images than needed and use gentle set points, large imaging gains, and low scan rates when imaging large and rough areas.

3.7 Using the instrument software, reduce the **Drive amplitude** to approximately 0.25 nm, and even lower when possible. Reduce the **Set Point** accordingly always to be less than the drive amplitude and **Acquire** test images. With a proper selection of the tip and imaging conditions, the drive amplitude can be reduced to $\sim 0.1 \text{ nm}$. However, be very careful when imaging with such a small amplitude over a rough surface topography could damage the tip.

NOTE: For a better vertical resolution, the drive amplitude should be smaller than the solution features that one is attempting to resolve. The smallest free amplitude that can realistically be reached is limited by the thermal noise associated with the cantilever and instrumental setup. One can qualitatively evaluate the signal-to-noise ratio while tuning the cantilever by analyzing the peak amplitude compared to the baseline noise.

3.8 Acquire single force curves starting from a tip-sample distance of 200 nm. Subsequently, reduce the tip-sample distance for the force curves to 50 nm, 10 nm, and finally 5 nm.

NOTE: Optimize the measurement conditions such that the amplitude in the retracted tip position is as low as possible ($< 0.25 \text{ nm}$); the phase shift in the retracted tip position is $\sim 90^\circ$; the excitation frequency (ν_{exc}) is equal or very close to the resonance frequency (ν_e), which simplifies the conversion of instrument observables to measured forces in the later steps; and the setpoint is low enough so that the phase shift (and amplitude) drops significantly (by $\sim 40\text{-}50\%$) within the last couple nanometers of the force measurement. The applied force can be further increased (setpoint decreased). The trade-off is that the tip is damaged more quickly in this process.

3.9. Make sure to withdraw the tip after the force curve acquiring has been stopped. If the tip remains engaged and close to the surface, it might drift towards and crash into the surface.

NOTE: **Figure 1** plots a 1D force curves for the muscovite-water system acquired in $[\text{NaCl}] = 10 \text{ mM}$ solution, specifically the phase (ϕ), amplitude (A), and deflection (δ) responses. At this stage,

these profiles should show evidence of the features that are aimed for in the 3D maps and manifested as oscillatory features that are mostly obvious in the phase curve. Note that the height coordinate for this raw data is arbitrary. Further details on data processing and analysis are provided in a later section.

4. Acquiring 3D force maps

NOTE: Finding the optimal parameters for 3D FFM measurements will depend on the sample surface, cantilever tip, and imaging solution. General guidelines are provided as a starting point but the appropriate parameters for each sample will require obtaining and analyzing datasets with various measurement conditions. The following steps show how to acquire the 3D force maps for the mineral water system. All of the parameters described in steps 4.2 – are set using the instrument software.

4.1. Perform all the steps as described in section 2 and 3.

4.2. Set the tip-sample distance (z) to 2–5 nm. This distance is sufficient to resolve interfacial solution features as the tip is close to the surface and, also allows the tip to equilibrate with the bulk solution when it retracts to the farthest position.

4.3. Set the Scan Area as 3 x 3 nm² or 10 x 10 nm², with a Resolution of 64 x 64 pixels² -128 x 128 pixels².

NOTE: Other applications such as bio-molecule imaging might require larger scan sizes in all three spatial dimensions.

4.4. Set the Rate of Force Curve Acquisition to 200–800 Hz, which corresponds to 15–120 s per 3D dataset. Ideally, decrease this number as much as possible to minimize image distortion and thermal drift of the tip, while maintaining a decent resolution in the z direction. For these scan rates and dimensions, 50–100 pix/nm are obtained in the z direction after processing the data, which is usually sufficient to resolve the interfacial solution structure.

4.5. As a starting point, choose a value for Set Point such that the phase shift routinely drops to ~50–60° in each force curve. The set point could be defined as low as 50% of the free amplitude. However, this especially depends on the type of sample being measured and will require trial and error. For example, using a low set point (high pressure) can damage the tip or deform the surface in the case of soft molecules. On the other hand, a high set point (low pressure) might not be sufficient to penetrate and probe the hydration layers.

4.6. Verify that the software is recording four key observables that are needed to analyze the amplitude modulated AFM data: tip height, amplitude, phase, and deflection. Note that multiple data channels could exist for tracking the tip height depending on the instrument and software. Since 3D FFM requires very high resolution, it is important to use the smoothest tip height profiles with the least overlain electronic noise from the instrument. In addition to recording these key

variables, other operating parameters and metadata are necessary to analyze and reconstruct the forces exerted on the tip (typically saved into your data file by default), as discussed in a later section.

NOTE: 3D FFM has been demonstrated in both amplitude modulated, and frequency modulated AFM modes. Regarding data quality and analysis, the two methods are equivalent. Accordingly, the preferred operation mode is left to the discretion and experience of the experimentalist. One possible advantage for the amplitude modulated mode is the stability of the tip over larger z distances that allows the user to obtain 3D data extending >10 nm into the solution. By comparison, one drawback of this mode concerns imaging soft molecules with relaxation timescales slower than the cantilever motion. The latter application presents an opportunity for FFM to investigate interfacial relaxation in soft material and viscous liquids. In these cases, the measured amplitude profiles might show hysteresis in the approach and retraction cycles, which creates uncertainty about the actual tip height.

5. Processing 3D force map data

NOTE: The following steps can be performed in the preferred data analysis software using in-house generated codes or alternatively using the data processing files provided in the **Supporting Information**.

5.1. Load the raw data into a preferred analysis software for calculations and visualization.

NOTE: The required observables for analysis are amplitude (A), phase shift (φ), and tip deflection (δ) as a function of the height displacement (z), as well as tip properties such as the resonance frequency (ν_e), spring constant (k), and quality factor (Q). Other operating parameters include the scan dimensions, scan rate, tip excitation frequency (ν_{exc}), and drive amplitude (A_0). The latter value is typically recorded in voltage units but can be readily converted to nanometers based on the calibration value obtained in Step 3.1.

5.2. Extract the equivalent topographic image from the 3D dataset by recording the farthest height displacement of the tip at each xy coordinate. Using this data, calculate the sample tilt by fitting straight lines to the average height profiles in both x and y scan directions. Even if the surface is atomically smooth such as mica, a sample tilt of several degrees is expected, and the corresponding height slope should be accounted for prior to data analysis.

NOTE. On most modern instruments, this step is automated for regular topographic imaging, but should be done manually for 3D FFM data. Obviously, this method should be slightly tweaked if the user measures more complex surfaces such as crystals with multiple-step edges.

5.3. Linearize the height displacement profiles. Recall that the tip in 3D FFM follows similar sinusoidal trajectories in every approach and retract cycle. However, the farthest extent of the tip varies depending on which crystallographic site it is landing on, and the recorded tip heights

are obviously not identical to the last significant figure. Accordingly, the height values measured in all the tip trajectories are discretized to obtain a single, linear z profile for all the force curves.

NOTE. The bin size depends on the measurement parameters and the length scale of the features of interest. For most applications, 0.2 Å is a sufficient height resolution. This value is more than ten times smaller than the size of a water molecule; using smaller bin sizes does not provide advantages and is in fact within the mechanical and electronic noise of the instrument.

5.4. Calculate the average observable values corresponding to the height bins for each individual force curve. This method produces a 3D volume of the phase/amplitude data that can be easily sliced and visualized in any direction.

NOTE: In principle, the force profiles from the tip approach and retraction should be similar. One could test whether it is more appropriate to use data from either or both depending on the specific sample. In particular, biomolecules and softer larger molecules could show hysteresis effects in the approaching / retracting cycles. In this case, the user is advised to modify the imaging conditions as described above.

5.5. Adjust the height profiles by accounting for the tip deflection. This step is optional and left for the discretion of the user. For example, with cantilevers having large spring constants (>200 N/m), the tip deflection in the dilute salt solution is typically less than <0.08 Å, which does not significantly influence the data.

NOTE: Based on the specific sample, the user can either 1) neglect the tip deflection for very stiff cantilevers after double-checking that their effect is negligible, 2) correct the tip height using the deflection profile averaged from the whole dataset, 3) correct the tip height for each individual force curve using the corresponding tip deflection data from that force curve. The latter option is intuitively the most “correct” and should be exercised when possible, but this approach often introduces more noise in the data that outweighs the merit of this correction.

5.6. Smooth the dataset using a 3D median filter. For most cases, this optional step reduces the noise without compromising the resolution. It is useful to keep a version of the un-filtered data as well for consistency checks during later analysis steps. Moreover, the user can explore more advanced filtering methods such as principal component analysis-based methods, which are readily available with most data processing software.

5.7 Save the processed results, as well as the useful metadata (measurement parameters important for transforming AFM observables to tip-sample force) into a data file that can be used for subsequent analysis.

NOTE: The three data processing files provided in the **Supporting Information** can be used to perform the functions listed in this section. The first file loads the raw 3D FFM data and creates an hdf5 file that includes the relevant data and metadata; this is simply a transfer of the data into a more user-friendly file that could be more readily accessed for processing. The second file

processes the raw data, according to the steps described above, by extracting the equivalent height image, linearizing the height displacement profiles, sorting the data values into the corresponding height bins, smoothing the dataset using a filter, and save the processed results into an output data file. The user can also activate some features to plot example force curves (raw and processed), xz/xy slices, and the correction for substrate tilt, as well as perform other post-processing consistency checks. These data processing scripts are user-friendly and annotated, showing the exact steps for users to tweak parameters and extract data from the raw instrument files.

REPRESENTATIVE RESULTS:

Figure 2A presents a schematic of 3D force mapping. Similar to other AFM techniques operating in amplitude modulated mode, an oscillating cantilever is scanned across the surface. In addition to the tip height at each coordinate, instrument observables such as phase shift and amplitude are collected as the tip approaches and retracts from the surface. The result is a 3D dataset of observables—notably the oscillation amplitude, phase shift, and tip deflection—that can be readily converted into a measurement of the force exerted on the tip. This method for the tip modulation is suitable for fast acquisition rates and produces reliable 3D data within a reasonable timescale of tens of seconds.

As a representative example, a 3D force map of a muscovite mica surface in contact with water is provided (**Figure 2B,C**). The data presented in terms of the force gradient experienced by the AFM tip (detailed explanation below) show lateral and vertical sub-nanometer features in three spatial dimensions. These features are ascribed to the interfacial solution structure and dissipate in the bulk solution, at heights beyond one nanometer from the surface. For a detailed description of the scientific significance and recent results from 3D FFM, the reader is referred to a review article by Fukuma and Garcia¹⁴. In this manuscript, we provide an experimental protocol for acquiring, processing, and analyzing 3D FFM data.

FIGURE AND TABLE LEGENDS:

Figure 1: 1D force curves. Example force curves acquired for muscovite mica in 10 mM NaCl solution showing data in terms of (A) φ , (B) A , and (C) δ . Scaling of z in nm is accurate, but $z = 0$ nm is an approximation.

Figure 2: 3D FFM scheme and representative data. (A) Schematic of 3D FFM data acquisition. Representative (B) xz and (C) xy data slices of the force gradient map obtained for muscovite mica in pure water.

Figure 3: Comparison of 3D FFM data with different tips. xz slices of 3D FFM data acquired for muscovite mica in 10 mM NaCl solution using (A) silicon AC55TS tip and (B) carbon USC-F5-k30-10 tip. (C) Average force profiles of the data sets obtained using the silicon tip (red) and carbon tip (blue).

Figure 4: Effect of tip blunting. (A) Average force profile from 3D FFM data set obtained for muscovite mica in pure water with increasingly blunted tip (blue, red, yellow, magenta, respectively). (B) Force gradients for the blue and red profiles in (A). (C) Image with exceedingly blunted tip still shows lattice resolution.

Figure 5: Force reconstruction from 3D FFM data acquired for muscovite mica in 10 mM NaCl solution. Comparison of (A) tip-sample interactions calculated using the Kuehnle equations (blue markers) as well as the Garcia equations including the first (solid, red), second (solid, yellow), and third (solid, magenta) force components, (B) tip-sample force gradient showing features corresponding to the solution structure.

Figure 6: Flow chart of 3D FFM data acquisition, processing, and analysis.

DISCUSSION:

Selecting the AFM tip

As with any AFM application, the key characteristics of the probe tip are the resonance frequency, cantilever size, tip radius, tip material, and spring constant. Almost all the 3D FFM literature to date has reported the use of stiff, high-frequency tips. The most common examples are silicon-based tips (e.g., AC55TS, PPP-NCH, Tap300-G, etc.) tips that can be utilized in their higher resonance modes¹⁴. Other research groups have opted for USC-F5-k30-10 carbon tips. Some important considerations are discussed below.

The cantilevers should be stiff, with spring constants $k > 1$ N/m. Otherwise, the tip will be subjected to large deflections and possibly adhere to the surface during each approaching and retracting cycle, instead of following the desired sinusoidal trajectory. In addition to tip deflection due to interactions with the surface, the solution structure itself might compromise the stability of tips with low spring constants, as the measured force gradients can exceed 0.1 N/m depending on the sample. In such cases, even if the tip can detect oscillatory features in the force profiles, the data would not be reliable. At the other extreme, tips that are too rigid might be incapable of detecting small features in the force profiles. The latter problem can be mitigated to some extent by operating at high resonance frequencies or extremely low drive amplitudes (< 0.1 nm) that are inaccessible to softer tips.

Cantilevers with higher resonance frequency ($\nu_0 > 1$ MHz in air) are more capable of resolving sub-nanometer, minor features in the force profiles. Recall that the minimum detectable force in AFM is given by:

$$F_{min} = \sqrt{\frac{4kk_BTB}{\pi\nu_0Q}} \quad (Eq. 1)$$

where k_B , T , B , ν_0 , and Q denote Boltzmann's constant, temperature, measurement bandwidth, resonance frequency, and quality factor of the cantilever resonance; respectively⁴¹.

In general, the options are either silicon tips that are assumed to have hydrophilic silicon dioxide termination in aqueous solutions or hydrophobic carbon tips. For this technique, hydrophilic tips are considered superior and more suitable for comparing the instrument data with existing theoretical models. However, note that silicon tips are more brittle than electron beam-deposited carbon tips, and should be handled very carefully when acquiring consecutive data sets.

Figure 3 compares force maps obtained on a muscovite mica surface in $[KCl] = 1$ mM using two different AFM tips. The hydrophilic AC55TS tip produces laterally resolved features templated by the underlying mica lattice (**Figure 3A**). By comparison, USC-F5-k30-10 tips with significantly lower spring constants can also resolve clear oscillations in the force curves. However, these hydrophobic tips measure a qualitatively different force map that shows a layered pattern with a spacing comparable to the size of a water molecule (**Figure 3B**). Interestingly, Seibert et al. determined that hydrophobic surfaces are likely to attract contaminants that render the results interpretation very challenging⁴². As an optimal solution, the Fukuma group has recommended the use of USC-F5-k30-10 tips that are sputter coated with silicon²⁴. This method cedes control over the tip radius but produces hydrophilic probes with an ideal range of resonance frequency and spring constant.

Regarding the tip size, the most used tips for this technique have nominal radii of 2–10 nm. For ultra-sharp tips (<2 nm), additional noise due to lateral tip oscillations can decrease image resolution. At the other extreme of a large “planar” tip, the force response is expected to be radically different due to fluid confinement between the two large surfaces; i.e., more comparable to surface force apparatus measurements.

To evaluate the effect of tip radius in the intermediate range relevant to 3D AFM force maps are acquired using a single tip that has been progressively blunted (**Figure 4A**). Notice that the oscillatory features gradually become less resolved (**Figure 4B**). While the peak positions do not change appreciably in this case, the magnitude of these features decreases. This effect is ascribed to the blunted tip detecting a convoluted signal from a large substrate area instead of sharp responses from distinct crystallographic sites. Interestingly, the blunted tip is still capable of producing lattice-resolution 2D images, even after the resolution in the height coordinate has been significantly compromised (**Figure 4C**). This presents a caution; a damaged tip could produce topographic images of the highest quality but still produce distorted 3D data.

In summary, the most favorable tips are stiff, sharp, and hydrophilic, with a high resonance frequency for improved sensitivity.

Data analysis

After the processing steps are completed, the measured observables can be converted into the force exerted on the tip at each voxel of the 3D dataset. This problem is discussed in a considerable body of literature using multiple approaches and assumptions^{43,44}. The common underlying feature in these methods is that the cantilever is considered as a driven harmonic oscillator where the cantilever and tip are reduced to an effective point mass:

$$F_{tot} = F_{ts} + \frac{A_0 k}{Q} \cos(2\pi v_{exc} t) - k\delta - \gamma \dot{\delta}$$

where F_{tot} is the total force acting on the tip, and the four terms on the right represent the tip-sample (ts) interactions, the driven harmonic oscillator force, the restoring force due to attachment of cantilever to a mechanical support, and the frictional force (γ denotes damping constant), respectively. Multiple formulations exist for solving this problem, although the fundamental physics is the same. In particular, the methods by Söngen et al. from the Kühnle research group⁴³ and Payam et al. from the Garcia research group⁴⁴ are highlighted here, which have been successfully implemented on 3D FFM data. The former approach gives:

$$\langle k_{ts} \rangle = k \left(1 - \left(\frac{v_{exc}}{v_e} \right)^2 \right) - \frac{A_0 k}{QA} \cos \phi \quad (Eq. 2)$$

For data acquired in amplitude modulated mode, the first term can be ignored since the cantilever oscillates at its resonance frequency. In reality, this term can be calculated for datasets where v_{exc} is not exactly identical to v_e , but its contribution is generally minimal. The imaging contrast is hence provided by $(\cos \phi)/A$. By comparison, the method from the Garcia group reconstructs the conservative force acting on the tip according to:

$$F_c(z) = 2k \int_z^\infty X dr + 2k \int_z^\infty \frac{\alpha A}{\sqrt{\pi(r-z)}} X dr - 2k \frac{\partial}{\partial z} \int_z^\infty \frac{A^{\frac{3}{2}}}{\sqrt{2(r-z)}} X dr \quad (Eq. 3)$$

$$X = \frac{A_0}{2QA} \cos \phi - \frac{1}{2} \left(\frac{v_0^2 - v_{exc}^2}{v_0^2} \right) \quad (Eq. 4)$$

where α is a constant, and the variables z , r , and v were used here instead of d , x , and ω in the original reference, respectively, for consistency with Equation 2 and the rest of this manuscript. Notice that the derivative of the first term in Equation 3 corresponds to the force gradient calculated in Equation 2. However, the second and third terms are negligible; in particular the contribution of the third term is dominant at high drive amplitudes (few nanometers) but significantly lower at typical 3D FFM imaging conditions (**Figure 5A**).

Depending on the sample and the choice of the tip, the oscillatory features are sometimes not clearly resolved in the force profiles, as they are overlain on the long-range interaction between the tip and the sample. These features are more clearly observed when plotting the force gradient, for instance, using Equation 2 (**Figure 5B**). Traditionally, the long-range interaction has been considered (or ignored) according to one of the following methods: (1) Qualitatively analyzing the oscillatory features in terms of the instrument observables, i.e., amplitude, phase, and frequency shift without transforming the data into a force-distance curve, and without accounting for the long-range interaction^{25,26,36}. This approach is a decent qualitative representation of the force gradient, which scales with $(\cos \phi)/A$ in amplitude-modulated mode. (2) Transforming the instrument observables into force or force gradient curves (using one of the two formulations described above) and studying the local oscillatory features semi-quantitatively while still ignoring the long-range background^{27,28,45}. This method is a decent first approximation

of the magnitude of the oscillatory features, and hence the degree of water ordering at the surface. (3) Subtracting the long-range tip-sample interaction using a function that is motivated by a physical rationale and ascribing the residual features to the interfacial solution structure. In principle, this method is the most quantitative and self-consistent. However, it predicates a fundamental knowledge of the nature and scaling of the tip-sample interactions. In earlier 3D FFM studies, this long-range background was subtracted using an exponential fit^{14,46}, similar to how the Debye-Hückel term is treated in surface force apparatus data. However, this approach did not produce good results for a variety of experimental systems. More recently, a rationale based on nanoscale hydrodynamics suggested a power-law scaling of this tip-sample interaction, which produced excellent results for the boehmite-water system⁴⁷. The authors suggest that the oscillatory motion of the AFM tip in the vicinity of a large planar surface leads to a “conservative” hydrodynamic lubrication force that scales according to $\langle k_{ts} \rangle = a(z + b)^{-3}$. Subtracting this long-range background revealed a clear patterning of the solution structure close to the interface. Further data is needed to validate this approach.

Data interpretation

The ability to resolve interfacial features with sub-nanometer 3D resolution is, by itself, an impressive technological feat. However, scientific progress from this technique will not be possible without important advances in data interpretation. We consider two questions:

Does the AFM tip influence the measured features, and how? In other words, how can one extrapolate information about the free substrate-solution interface based on measurements using an AFM tip?

The simplest approach to this problem is a direct transformation between water density distribution (ρ) and force profiles using the solvent-tip approximation (STA)⁴⁸:

$$F(z) = \frac{k_B T}{\rho(z)} \frac{d\rho(z)}{dz}$$

The rationale for this method is straightforward: the AFM tip is assumed to behave like a water molecule, hence experiencing energy minima in locales of high water density close to the surface. Accordingly, the STA is mostly plausible for sharp, hydrophilic tips whose tightly bound hydration layer is effectively part of the tip, which is in line with previous work where 1D force curves were acquired using ultrasharp tips of different hydrophilicity⁴⁹. The STA model has been applied to water density maps obtained from molecular simulations on mineral-solution interfaces. In some cases, the STA model has shown decent qualitative agreement with 3D FFM measurements²³.

Nevertheless, more rigorous approaches are needed to account for the complexity of the tip size, chemistry, physical shape, as well as water confinement between the tip and the sample. Recently, Miyazawa et al. presented an “extended-STA” model wherein the tip chemistry is varied in molecular dynamics simulations (carbonate, calcium, or hydroxyl terminations) which resulted in drastic changes to the hydration structure at the interface⁵⁰. Another study from our group used molecular dynamics simulations to survey the effect of tip size, tip-sample specific

interactions, and tip chemistry, with each variation capturing an additional level of complexity observed in the experimental data⁴⁷.

How can one de-convolute the two main components of the measured force: tip-substrate colloidal forces and tip-solution hydration forces?

The full answer to this question is beyond current theoretical models. Most studies have ignored the long-range interaction whose detailed physical nature is not completely clear and focused on the short-range oscillatory features. If achieved, a deeper understanding of the tip-sample interactions can become an asset of 3D FFM as it provides insights into colloidal interactions in addition to producing a more systematic and self-consistent analysis of the interfacial solution structure.

Ideally, one would delineate the dependence of forces, such as van der Waals, electrostatic, and hydrodynamic interactions, on local solution structure, patterns in the charge distribution, as well as other variables close to the interface where traditional models break down. The approach of analyzing the background as arising from the “conservative” hydrodynamic lubrication force (mentioned above) is a promising step in this direction that requires further investigation⁴⁷. The schematics for 3D FFM data acquisition, processing, and analysis is shown in **Figure 6**.

To date, 3D FFM has been applied to multiple mineral-solution systems. In some cases, the results have been validated by molecular dynamics simulations, while in other cases questions about the role of the AFM tip have proven challenging^{24,25,29,51}. As more details regarding data interpretation are ironed out, the next important steps will be to venture beyond these early benchmarking experiments and generalize 3D FFM to other applications in the wide range of scientific domains for which interfacial structure is an important factor. We anticipate that this technique will play a leading role in solving problems related to fundamentals of interfacial solution structure, surface chemistry, and colloidal physics, which in turn holds great promise for a deeper understanding in a multitude of research fields including electrochemistry, catalysis, geochemistry, materials science, biochemistry and biology.

ACKNOWLEDGMENTS

We thank Dr. Marta Kocun (Asylum Research), Dr. Takeshi Fukuma (Kanazawa), Dr. Ricardo Garcia (CSIC Madrid), Dr. Angelika Kühnle (Bielefeld), Dr. Ralf Bechstein (Bielefeld), Sebastien Seibert (Bielefeld), and Dr. Hiroshi Onishi (Kobe) for useful discussions.

Development of the 3D FFM experimental protocol was supported as part of IDREAM (Interfacial Dynamics in Radioactive Environments and Materials), an Energy Frontier Research Center funded by the U.S. Department of Energy (DOE), Office of Science (SC), Office of Basic Energy Sciences (BES). Development of the 3D FFM data analysis code was supported by the Laboratory Directed Research and Development Program (LDRD) at Pacific Northwest National Laboratory (PNNL) through the Linus Pauling Distinguished Postdoctoral Fellowship program to which E.N. is grateful for support. Development of the 3D FFM measurement capability was carried out at PNNL with support from the BES Division of Materials Science and Engineering, Synthesis and

Processing Sciences Program. PNNL is a multiprogram national laboratory operated for DOE by Battelle Memorial Institute under contract no. DEAC05-76RL0-1830.

DISCLOSURES

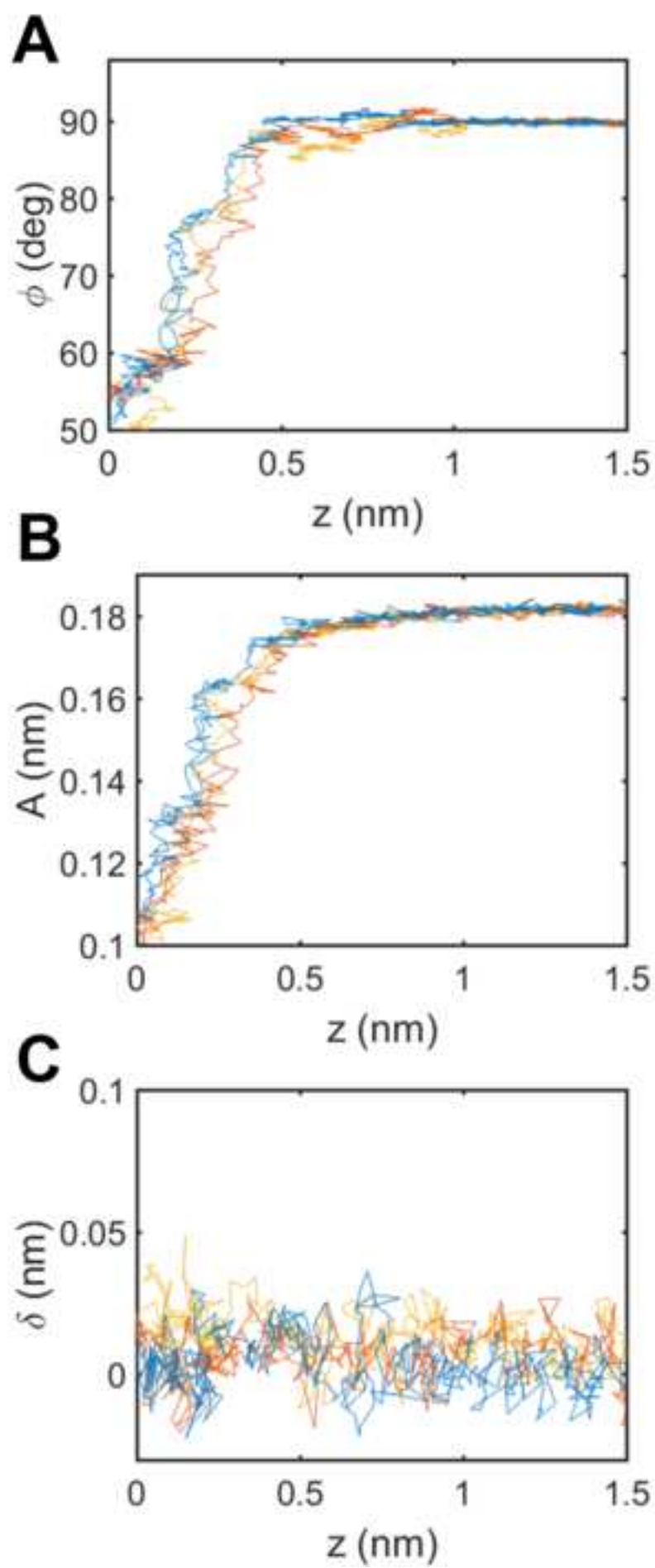
The authors declare no competing financial interests or other conflicts of interest.

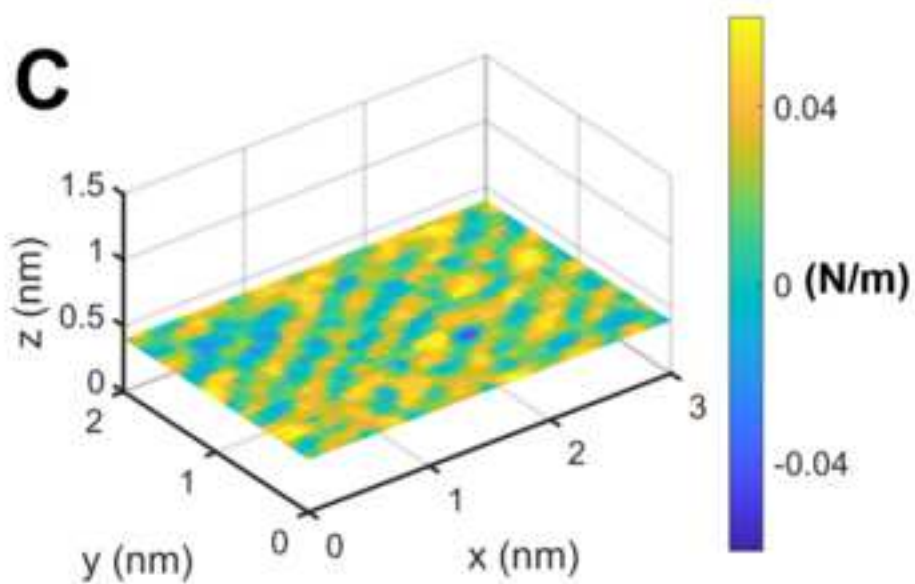
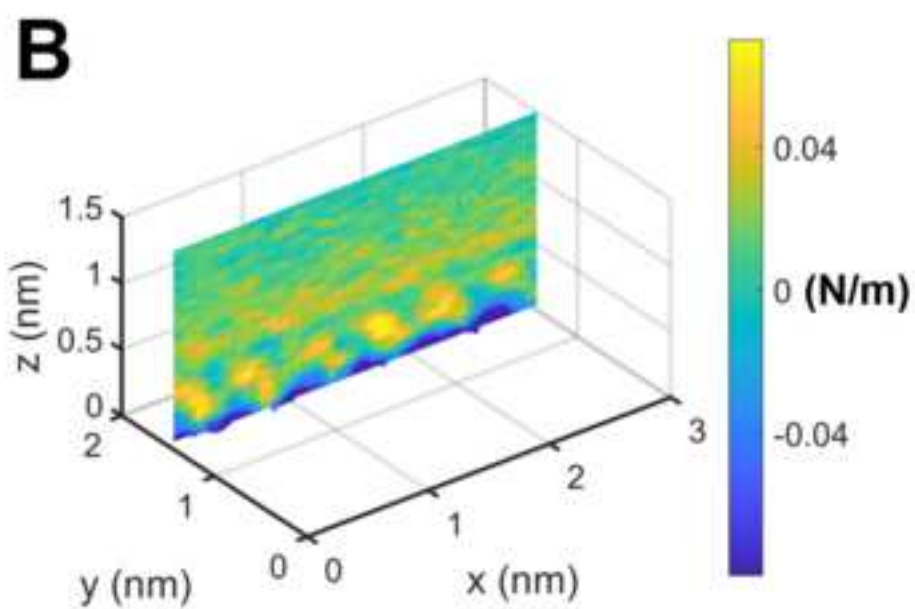
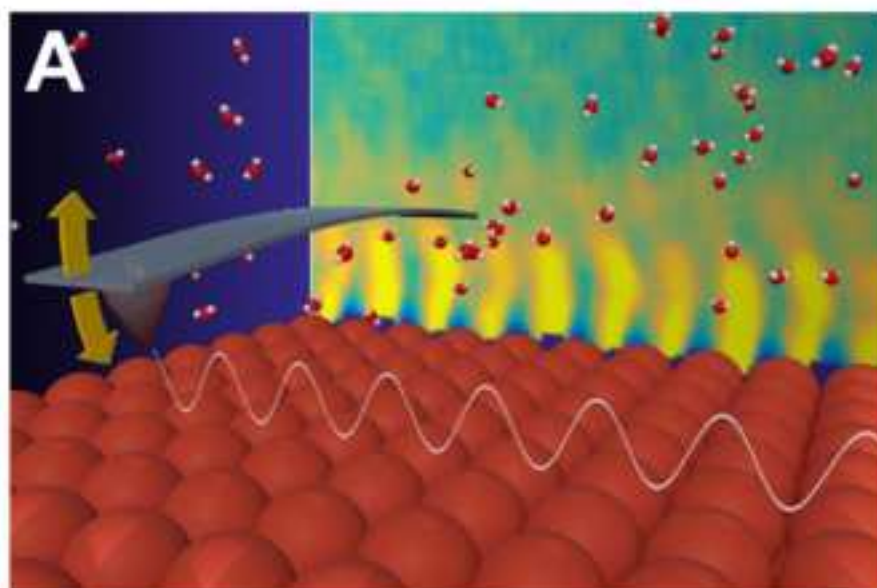
REFERENCES

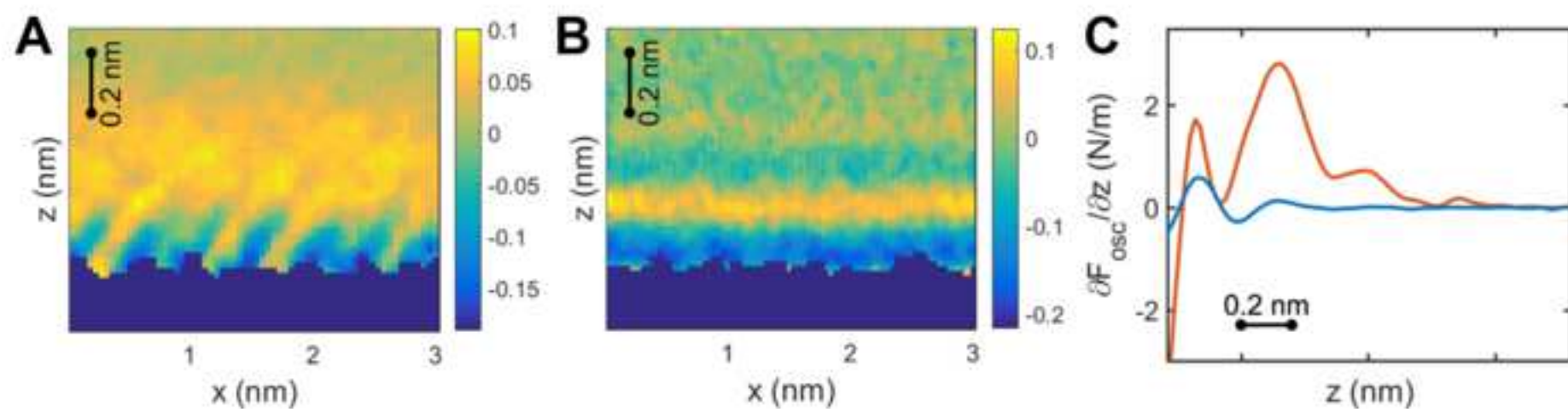
- 1 Israelachvili, J. N. *Intermolecular and Surface Forces*. Third edition. Academic Press. (2011).
- 2 Israelachvili, J. N., Pashley, R. M. Molecular layering of water at surfaces and origin of repulsive hydration forces. *Nature*. **306** (1983).
- 3 Bentley, C. L., Kang, M., Unwin, P. R. Nanoscale surface structure-activity in electrochemistry and electrocatalysis. *Journal of American Chemical Society*. **141**, 2179-2193 (2019).
- 4 Bourg, I. C., Lee, S. S., Fenter, P., Tournassat, C. Stern layer structure and energetics at mica–water interfaces. *Journal of Physical Chemistry C*. **121**, 9402-9412 (2017).
- 5 Lee, S. S., Fenter, P., Nagy, K. L., Sturchio, N. C. Real-time observation of cation exchange kinetics and dynamics at the muscovite-water interface. *Nature Communications*. **8**, 15826 (2017).
- 6 Suo, L. et al. “Water-in-salt” electrolyte makes aqueous sodium-ion battery safe, green, and long-lasting. *Advanced Energy Materials*. **7**, 1701189 (2017).
- 7 Magnussen, O. M., Gross, A. Toward an atomic-scale understanding of electrochemical interface structure and dynamics. *Journal of American Chemical Society*. **141**, 4777-4790 (2019).
- 8 Chen, J. et al. Building two-dimensional materials one row at a time: Avoiding the nucleation barrier. *Science*. **362**, 1135-1139 (2018).
- 9 Nakouzi, E. et al. Impact of solution chemistry and particle anisotropy on the collective dynamics of oriented aggregation. *ACS Nano*. **12**, 10114-10122 (2018).
- 10 De Yoreo, J. J. et al. Crystallization by particle attachment in synthetic, biogenic, and geologic environments. *Science*. **349**, aaa6760 (2015).
- 11 Liu, L. et al. Connecting energetics to dynamics in particle growth by oriented attachment using real-time observations. *Nature Communications*. **11**, 1045 (2020).
- 12 Lee, J. et al. Mechanistic understanding of the growth kinetics and dynamics of nanoparticle superlattices by coupling interparticle forces from real-time measurements. *ACS Nano*. **12**, 12778-12787 (2018).
- 13 Lee, J. et al. Interplay between short- and long-ranged forces leading to the formation of Ag nanoparticle superlattice. *Small*. **15**, 1901966 (2019).
- 14 Fukuma, T., Garcia, R. Atomic- and molecular-resolution mapping of solid-liquid interfaces by 3D atomic force microscopy. *ACS Nano* **12**, 11785-11797 (2018).
- 15 Herruzo, E. T., Asakawa, H., Fukuma, T., Garcia, R. Three-dimensional quantitative force maps in liquid with 10 piconewton, angstrom and sub-minute resolutions. *Nanoscale*. **5**, 2678-2685 (2013).
- 16 Zhang, X. et al. Direction-specific interaction forces underlying zinc oxide crystal growth by oriented attachment. *Nature Communications*. **8**, 835 (2017).

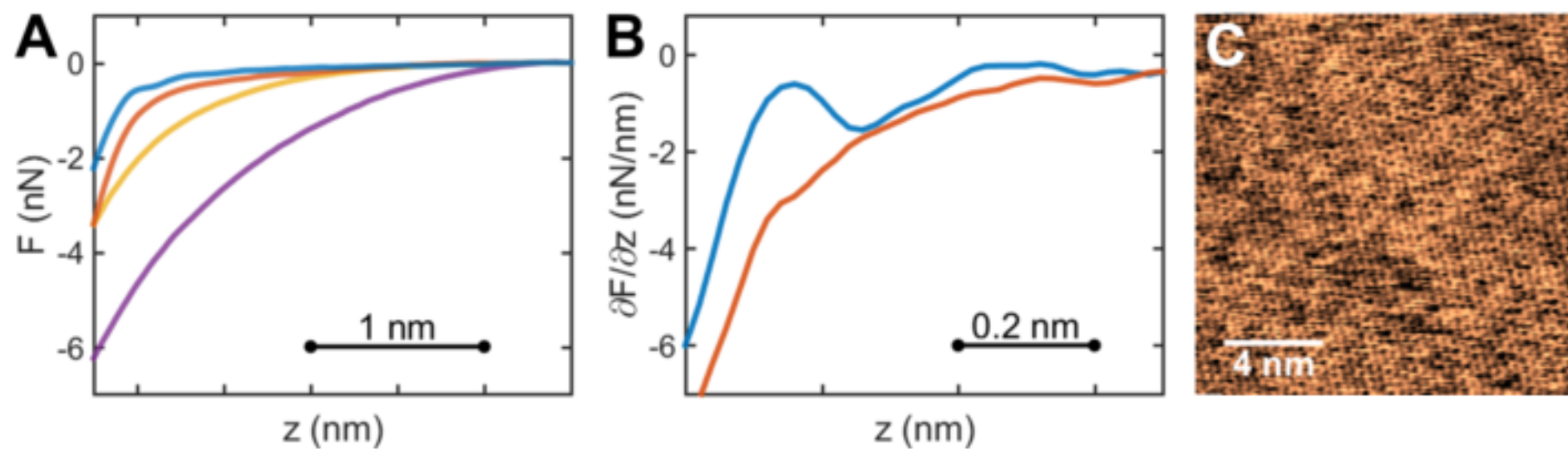
- 17 Li, D. et al. Trends in mica–mica adhesion reflect the influence of molecular details on long-range dispersion forces underlying aggregation and coalignment. *Proceedings of the National Academy of Science U. S. A.* **114**, 7537-7542 (2017).
- 18 Eaton, P., West, P. *Atomic Force Microscopy*. Oxford University Press (2018).
- 19 Fukuma, T., Kobayashi, K., Matsushige, K., Yamada, H. True atomic resolution in liquid by frequency-modulation atomic force microscopy. *Applied Physics Letters*. **87**, 034101 (2005).
- 20 Miller, E. J. et al. Sub-nanometer resolution imaging with amplitude-modulation atomic force microscopy in liquid. *Journal of Visualized Experiments*. (118) e54924 (2016).
- 21 Legg, B. A. et al. Visualization of aluminum ions at the mica water interface links hydrolysis state-to-surface potential and particle adhesion. *Journal of the American Chemical Society*. **142**, 6093-6102 (2020).
- 22 Fukuma, T., Ueda, Y., Yoshioka, S., Asakawa, H. Atomic-scale distribution of water molecules at the mica-water interface visualized by three-dimensional scanning force microscopy. *Physical Review Letters*. **104**, 016101 (2010).
- 23 Fukuma, T. et al. Mechanism of atomic force microscopy imaging of three-dimensional hydration structures at a solid-liquid interface. *Physical Review B*. **92**, 155412 (2015).
- 24 Miyazawa, K. et al. A relationship between three-dimensional surface hydration structures and force distribution measured by atomic force microscopy. *Nanoscale*. **8**, 7334-7342 (2016).
- 25 Songen, H. et al. Chemical identification at the solid-liquid interface. *Langmuir* **33**, 125-129 (2017).
- 26 Songen, H. et al. Resolving point defects in the hydration structure of calcite (10.4) with three-dimensional atomic force microscopy. *Physical Review Letters*. **120**, 116101 (2018).
- 27 Martin-Jimenez, D., Chacon, E., Tarazona, P., Garcia, R. Atomically resolved three-dimensional structures of electrolyte aqueous solutions near a solid surface. *Nature Communications*. **7**, 12164 (2016).
- 28 Martin-Jimenez, D., Garcia, R. Identification of single adsorbed cations on mica-liquid interfaces by 3D force microscopy. *Journal of Physical Chemistry Letters*. **8**, 5707-5711 (2017).
- 29 Miyazawa, K., Watkins, M., Shluger, A. L., Fukuma, T. Influence of ions on two-dimensional and three-dimensional atomic force microscopy at fluorite-water interfaces. *Nanotechnology*. **28**, 245701 (2017).
- 30 Fenter, P., Kerisit, S., Raiteri, P., Gale, J. D. Is the calcite–water interface understood? Direct comparisons of molecular dynamics simulations with specular X-ray reflectivity data. *Journal of Physical Chemistry C*. **117**, 5028-5042 (2013).
- 31 Pintea, S., de Poel, W., de Jong, A. E. F., Felici, R., Vlieg, E. Solid-liquid interface structure of muscovite mica in SrCl₂ and BaCl₂ solutions. *Langmuir*. **34**, 4241-4248 (2018).
- 32 Garcia, N., Raiteri, P., Vlieg, E., Gale, J. Water structure, dynamics and ion adsorption at the aqueous {010} brushite surface. *Minerals*. **8**, 334 (2018).
- 33 Bracco, J. N. et al. Hydration structure of the barite (001)–water Interface: Comparison of X-ray reflectivity with molecular dynamics simulations. *Journal of Physical Chemistry C*. **121**, 12236-12248 (2017).
- 34 Tuladhar, A., Piontek, S. M., Borguet, E. Insights on interfacial structure, dynamics, and proton transfer from ultrafast vibrational sum frequency generation spectroscopy of the alumina(0001)/water interface. *Journal of Physical Chemistry C*. **121**, 5168-5177 (2017).

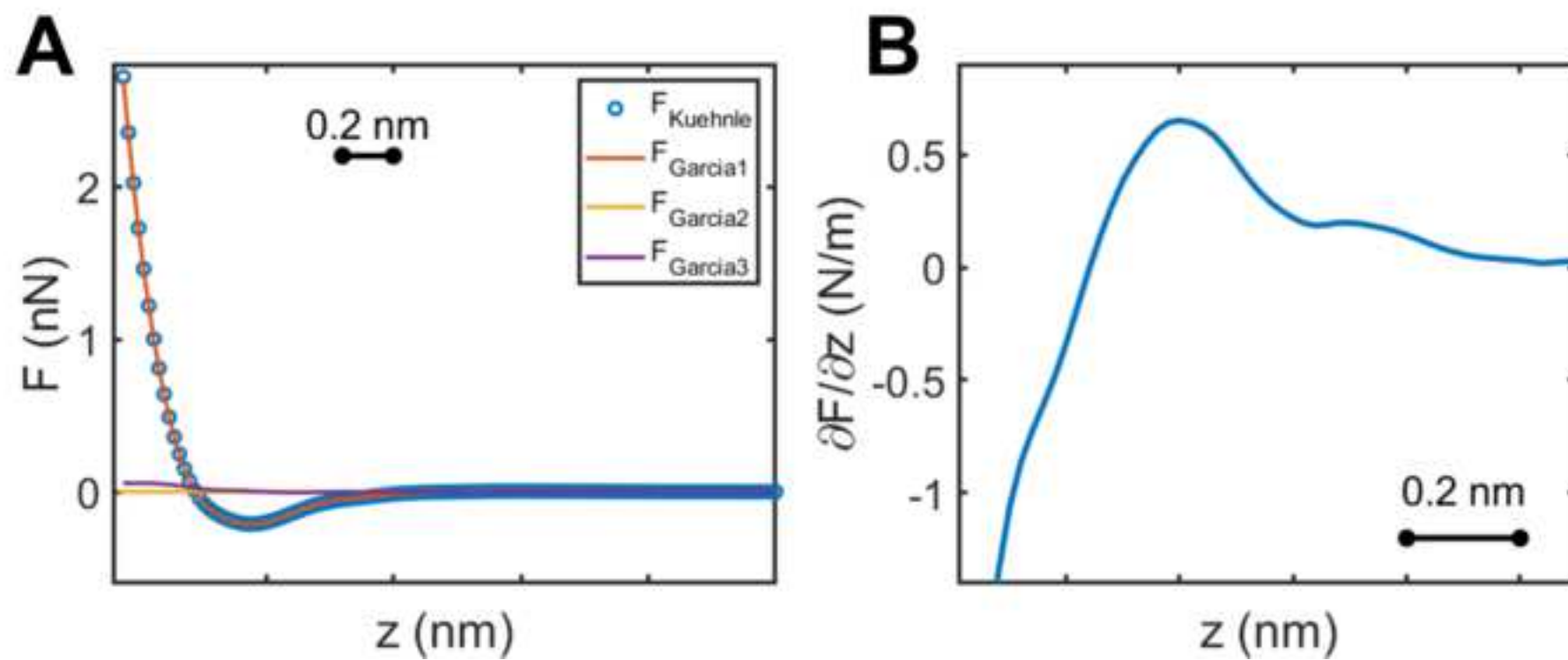
- 35 Dewan, S., Yeganeh, M. S., Borguet, E. Experimental correlation between interfacial water structure and mineral reactivity. *Journal of Physical Chemistry Letters*. **4**, 1977-1982 (2013).
- 36 Spijker, P. et al. Understanding the interface of liquids with an organic crystal surface from atomistic simulations and AFM experiments. *Journal of Physical Chemistry C*. **118**, 2058-2066 (2014).
- 37 Kerisit, S., Okumura, M., Rosso, K., Machida, M. Molecular simulation of cesium adsorption at the basal surface of phyllosilicate minerals. *Clays and Clay Minerals*. **64**, 389-400 (2016).
- 38 Kerisit, S. N., De Yoreo, J. J. Effect of hydrophilicity and interfacial water structure on particle attachment. *Journal of Physical Chemistry C*. **124**, 5480-5488 (2020).
- 39 Willemsen, J. A. R., Myneni, S. C. B., Bourg, I. C. Molecular dynamics simulations of the adsorption of phthalate esters on smectite clay surfaces. *Journal of Physical Chemistry C*. **123**, 13624-13636 (2019).
- 40 Voïtchovsky, K. High-resolution AFM in liquid: What about the tip? *Nanotechnology*. **26**, 100501 (2015).
- 41 Fukuma, T., Onishi, K., Kobayashi, N., Matsuki, A., Asakawa, H. Atomic-resolution imaging in liquid by frequency modulation atomic force microscopy using small cantilevers with megahertz-order resonance frequencies. *Nanotechnology*. **23**, 135706 (2012).
- 42 Seibert, S., Klassen, S., Latus, A., Bechstein, R., Kuhnle, A. Origin of ubiquitous stripes at the graphite–water interface. *Langmuir*. **36**, 7789–7794 (2020).
- 43 Songen, H., Bechstein, R., Kuhnle, A. Quantitative atomic force microscopy. *Journal of Physics: Condensed Matter*. **29**, 274001 (2017).
- 44 Payam, A. F., Martin-Jimenez, D., Garcia, R. Force reconstruction from tapping mode force microscopy experiments. *Nanotechnology*. **26**, 185706 (2015).
- 45 Araki, Y., Sekine, T., Chang, R., Hayashi, T., Onishi, H. Molecular-scale structures of the surface and hydration shell of bioinert mixed-charged self-assembled monolayers investigated by frequency modulation atomic force microscopy. *RSC Advances*. **8**, 24660-24664 (2018).
- 46 Asakawa, H., Yoshioka, S., Nishimura, K.-i., Fukuma, T. Spatial distribution of lipid headgroups and water molecules at membrane water interfaces visualized by three-dimensional scanning force microscopy. *ACS Nano*. **10**, 9013–9020 (2012).
- 47 Nakouzi, E. et al. Moving beyond the solvent-tip approximation to determine site-specific variations of interfacial water structure through 3D force microscopy. *Journal of Physical Chemistry C*. **125**, 1282–1291 (2020).
- 48 Watkins, M., Reischl, B. A simple approximation for forces exerted on an AFM tip in liquid. *Journal of Chemical Physics*. **138**, 154703 (2013).
- 49 Kaggwa, G. B., Nalam, C. P., Kilpatrick, J. I., Spencer, N. D., Jarvis, S. P. Impact of hydrophilic/hydrophobic surface chemistry on hydration forces in the absence of confinement. *Langmuir*. **28**, 6589–6594 (2012).
- 50 Miyazawa, K. et al. Tip dependence of three-dimensional scanning force microscopy images of calcite–water interfaces investigated by simulation and experiments. *Nanoscale*. **12**, 12856–12868 (2020).
- 51 Umeda, K. et al. Atomic-resolution three-dimensional hydration structures on a heterogeneously charged surface. *Nature Communications*. **8**, 2111 (2017).

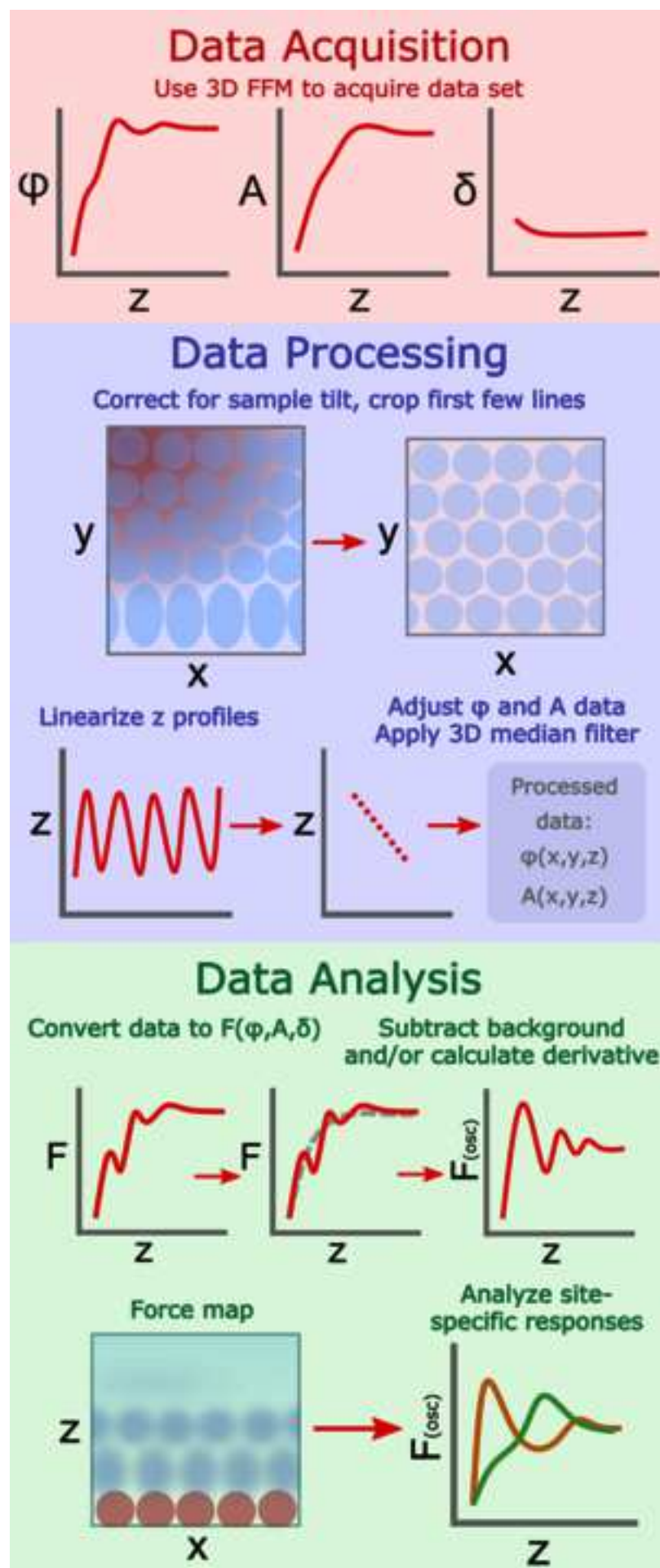












Name of Material/Equipment	Company	Catalog Number	Comments/Description
AC55TS AFM tip	Olympus		
Cypher VRS Atomic Force Microscope	Asylum Research		
PPP-NCH AFM tip	Nanosensors		
Tap300-G AFM tip	Budget Sensors		
USC-F5-k30-10 AFM tip	Nanoworld		

(Note only one of the AFM tip options is required)

Visualizing Solution Structure at Solid-Liquid Interfaces Using Three-Dimensional Fast Force Mapping

Editorial comments:

1. Please take this opportunity to thoroughly proofread the manuscript to ensure that there are no spelling or grammar issues. Please define all abbreviations at first use.

All abbreviations are defined at first use.

2. Please provide an email address for each author, and specify who the corresponding author is.

The email addresses have been provided. There are two co-corresponding authors: Elias Nakouzi and James De Yoreo

3. Please provide a 10-50-word Summary (before the abstract) to clearly describe the protocol and its applications in complete sentences: "Here, we present a protocol to ..."

This section has been added.

4. Please revise the following lines to avoid overlap with previously published work: 36-38; 98-99

These statements have been modified.

5. For in-text formatting, corresponding reference numbers should appear as numbered superscripts after the appropriate statement(s), but before punctuation.

Reference numbers have been relocated to before punctuation.

6. Please roll the Method Description into the representative results.

The dataset presented in the Method Description was moved to the Representative Results section.

7. JoVE cannot publish manuscripts containing commercial language. This includes trademark symbols (™), registered symbols (®), and company names before an

instrument or reagent. Please remove all commercial language from your manuscript (text, figure legends, figures, tables) and use generic terms instead. All commercial products should be sufficiently referenced in the Table of Materials and Reagents.

For example: AmplnVOLS on Asylum Research instruments; AC55TS (Olympus); PPP-NCH (NanoSensors) or Tap300-G (BudgetSensor) tips; USC-F5-k30-10 (NanoWorld); Matlab etc

We have removed all the instrument-specific mentions from the AFM company (GetReal and AmpINVOLS as pertaining to this particular manufacturer).

However, the AFM tips cannot be referred to generically, as they are a key part of the protocol and a large section is dedicated to parsing out the differences between the tips, including with discussions and representative data. This is in many ways similar to mentioning the tip brand in the Methods section of other manuscripts. In this case, particularly, it is not possible to have a clear discussion on the role of different tip properties without naming the tips.

8. Please number your steps as 1 (section), 1.1. (step or sub-section), 1.1.1. (steps), 1.1.1.1. Leave one-line spacing between all steps and notes and highlight up to three pages of protocol text to indicate what should be filmed.

The “steps” have been renamed to 1.1 format.

The protocol is 4 sections. I recommend that Sections 1 and 2 be filmed but only briefly, as they are mostly pertinent to standard high resolution AFM imaging (Miller, E. J. et al. Sub-nanometer Resolution Imaging with Amplitude-modulation Atomic Force Microscopy in Liquid. Journal of Visualized Experiments, e54924 (2016))

Most of the filming would preferably show Sections 3 and 4 of the Protocols.

9. Please revise the text, especially in the protocol, to avoid the use of any personal pronouns (e.g., "we", "you", "our" etc.).

The use of personal pronouns has been reduced considerably and is now down to only a few instances (not in protocol part).

10. Please note that your protocol will be used to generate the script for the video and must contain everything that you would like shown in the video. Please add more details to your protocol steps. Please ensure you answer the “how” question, i.e., how is the step performed? Alternatively, add references to published material specifying how to perform the protocol action. Please add more specific details (e.g., button clicks for software actions, numerical values for settings, etc) to your protocol steps. There should be enough

detail in each step to supplement the actions seen in the video so that viewers can easily replicate the protocol. For example, how will you zero the deflection signal and measure the cantilever spring constant in air, etc. If these aspects are not the main focus of the protocol, consider citing references in which this will be described and/or include steps to include in the video so that readers/viewers of different levels of experience will understand how to execute this protocol.

To successfully operate this technique, a basic level of prior knowledge of modern AFM instruments is expected. As such, we have referred the reader to another JoVE paper to avoid redundancy of re-writing the basic protocol for AFM high resolution imaging:

*“A pre-requisite for implementing 3D FFM on a particular sample, is the ability to obtain topographic images with the desired spatial resolution. For a detailed experimental protocol on high-resolution AFM imaging, the reader **is referred** to a recent manuscript by Miller et al²⁰. Most of the recommendations in that protocol are applicable, and necessary, for 3D FFM. In the following, we briefly highlight the main steps for high-resolution imaging, but focus on specific considerations for 3D FFM.”*

However, the steps presented here are indeed self-sufficient. We have added further details to the following steps based on your recommendation.

Step 1.5 ... Generally, this step is automated on most modern microscopes by recording the thermal fluctuations of the cantilever, and fitting the first resonance peak to a simple harmonic oscillator model.

Step 3.1 ... Again, this step is automated on most modern microscopes.

Step 3.3 ... Typically, this is done by defining a setpoint amplitude that is approximately ~70% of the free amplitude. As the tip approaches the surface, the amplitude drops until it reaches the setpoint value and is thus determined to be engaged at the surface.

Step 3.7 ... Reduce the drive amplitude as much as possible, reduce the setpoint accordingly so that it is always less than the drive amplitude, and acquire test images.

Step 3.8 ... drops significantly (by ~40-50%) within the last couple nanometers of the force measurement

Step 3.8 ... If the tip remains engaged and close to the surface, it might drift towards and crash into the surface.

11. Please separate the representative results section and include this after the protocol before the figure and table legends section. The Discussion section will follow the legends section. Please have both representative results and discussion sections in paragraph style.

We have followed this formatting. Please note that the Discussion section is split into sub-sections for the most clarity and detailed description.

12. Please reference the supplemental coding files in the text to indicate when and how these would be useful.

The section titled “Data Processing” describes the use of the supplemental coding files. We have added further details for clarity.

“The first file loads the raw 3D FFM data and creates an hdf5 file that includes the relevant data and metadata; this is simply a transfer of the data into a more user-friendly file that could be more readily accessed for processing. The second file processes the raw data according to the steps described above, by extracting the equivalent height image, linearizing the height displacement profiles, sorting the data values into the corresponding height bins, smoothing the dataset using a filter, and save the processed results into an output datafile.”

13. Please include a Disclosures section, providing information regarding the authors’ competing financial interests or other conflicts of interest. If authors have no competing financial interests, then a statement indicating no competing financial interests must be included.

We have added the following sentence as requested: “The authors declare no competing financial interests or other conflicts of interest.”

14. Please remove the titles and Figure Legends from the uploaded figures. The legends should appear only in the Figure and Table Legends section after the Representative Results. Please use only uppercase letters for figure panels.

The Figure Legends were moved to the new section, figure titles were added, and the letters in the panels were changed to uppercase.

15. Please include a scale bar for all images taken with a microscope to provide context to the magnification used. Define the scale in the appropriate Figure Legend.

The scale bar is added to Figure 4c as requested. The other figures that show images already show the scaling on the figure axes.

16. Please ensure that the references appear as the following: [Lastname, F.I., LastName, F.I., LastName, F.I. Article Title. Source (*italics*). Volume (**bold**) (Issue), FirstPage–LastPage (YEAR).] For more than 6 authors, list only the first author then et al. Please include volume and issue numbers for all references. Please do not abbreviate journal names; use title case for all journal names.

The references have been tweaked to comply with your recommended format.

Reviewer comments:

We thank the reviewer for the positive assessment of our manuscript. We have made all the modifications suggested by the reviewer. These changes have clarified several key points; the manuscript is now improved.

1. Section 2.1: There is mention of pre-wetting the tip to avoid air bubbles. While important, it might be helpful to also recommend rinsing the area of the tip and the sample to be immersed in liquid with some experimental solution to limit as much as possible contamination from the environment. Perhaps more generally, high-resolution 2D AFM and 3D FFM is likely to be particularly sensitive to Interface contamination by organics or residual contaminants (see e.g. <https://www.nature.com/articles/ncomms12164>) so a small discussion around this issue and how to identify/root it out would be helpful.

We have added Step 1.2: “Clean the cantilever holder with water and isopropanol solvents as well.”

We have also expanded Step 2.2 and cited the mentioned paper:

“Rinse the sample with the imaging solution and then add ~100 µL of the same imaging solution onto the mica surface.

- Note: As with any other AFM measurement, having a clean surface is very critical for obtaining reliable 3D data, as the interface is particularly sensitive contamination by organics and other residues.^{27”}

2. Section 3.4: It may be worth mentioning explicitly that the phase should be centred at 90 degrees for consistency with the harmonic oscillator model that is used later on in the analysis. Since the phase can be offset arbitrarily, there is some discrepancy on where it is centred by default between different AFM manufacturers.

We have made the following modification: “center the phase shift at 90 degrees as in Step 3.2”

3. Section 3.7: There is mention that the amplitude to be used should be as small as possible, typically smaller than the size of a water molecule (0.25nm). In practice, the characteristics of the cantilever will determine what is the smallest amplitude that can realistically be reached, considering the thermal noise as the ultimate limit. This is partly addressed later on in terms of minimal force that can be measured, but a few comments

around the problem/limitation of thermal noise for the choice of cantilever would be helpful here.

We have added the following note to Step 3.7:

- **“Note: The smallest free amplitude that can realistically be reached is limited by the thermal noise associated with the cantilever and instrumental setup. One can qualitatively evaluate the signal-to-noise ratio while tuning the cantilever by analyzing the peak amplitude compared to the baseline noise.”**

4. Section 4, Operating mode: Linked to the previous point, the question of measurement timescale and relaxation is linked that of cantilever stiffness, size and thermal noise as well as hydrodynamic drag as the cantilever moves fast up and down. This may actually be an opportunity for FFM to investigate interfacial relaxation in soft material and viscous liquids, but it deserves a comment here. It may also be linked up with the discussion about selecting the correct spring constant later on in the paper.

We have added the following statement: **“The latter application presents an opportunity for FFM to investigate interfacial relaxation in soft material and viscous liquids.”**

5. Discussion section on Tip Chemistry: The question of hydrophilic vs hydrophobic tip is a difficult one because immersed hydrophobic surfaces are likely to attract contamination rendering result interpretation potentially time-dependent and challenging (see e.g. <https://www.nature.com/articles/ncomms12164>, <https://pubs.acs.org/doi/abs/10.1021/acs.langmuir.0c00748>). Focusing on solvophilic tips (as the authors do) seems like the best way forward to ensure straightforward result interpretation.

Thanks for reminding us of this very interesting paper. We had just been discussing these fascinating results in our group meetings. We have added the following statement: **“Interestingly, Seibert et al. determined that hydrophobic surfaces are likely to attract contaminants that render the results interpretation very challenging.”⁴²**

6. Discussion section on Tip Radius: There is an important point to be made here, and that also links up with the question of data interpretation (STA). The following paper examined the dependence of the tip chemistry on the resulting oscillatory profiles measured at interfaces and it seems that if the tip is sharp enough, then the profile measured is completely dominated by the solvation structure of the interface, not that of the tip: Kaggwa, G. B., Nalam, P. C., Kilpatrick, J. I., Spencer, N. D., & Jarvis, S. P. (2012). Impact of Hydrophilic/Hydrophobic Surface Chemistry on Hydration Forces in the

Absence of Confinement. Langmuir, 28(16), 6589-6594. <http://doi.org/doi:10.1021/la300155c>

In my view, this goes some way towards justifying sharp tips and the STA.

We have added the following phrase:

“Accordingly, the STA is mostly plausible for sharp, hydrophilic tips whose tightly bound hydration layer is effectively part of the tip, which is in line with previous work where 1D force curves were acquired using ultrasharp tips of different hydrophilicity.⁴⁹”

7. Data processing and the use of a median filter: while using filters is often helpful to remove noise, it can also be controversial and subjective. It might be worth mentioning more 'intelligent' filtering using e.g. a principal component analysis (in-built function in most data processing software such as Igor Pro, Matlab etc) which can provide a rational basis for filtering based on objective trends.

We have added the following statement:

“Moreover, the user can explore more advanced filtering methods such as principal component analysis-based methods which are readily available with most data processing software.”

8. Data analysis: The authors mention the harmonic oscillator model which underpins much AFM data interpretation. One of the key underlying approximation is that of the point mass where the whole cantilever and tip is reduced to an effective point mass (for better or worse). There is much discussion about this in the literature and while a lengthy digression on the topic would be a distraction here, a short comment would be helpful.

We have added this phrase for clarity. The already cited references cover this topic well.
“The common underlying feature in these methods is that the cantilever is considered as a driven harmonic oscillator **where the cantilever and tip are reduced to an effective point mass.**”

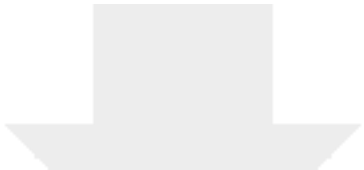
9. Final point of the discussion: There a good discussion about the different forces at play, their respective range and difficulty to disentangle the different contributions. I believe this is actually an opportunity for FFM since it allows for multiple sets of data in comparable conditions where only one parameter is changed. To date, such studies have been challenging due to the small amount of curves collected and the difficulty to compare reliably curves acquired over a particular location. FFM enables statistical approaches and could help tackle this issue across the field of AFM as a whole.

We definitely agree with the assessment of the opportunities offered by 3D FFM and have hence stated that: “If achieved, a deeper understanding of the tip-sample interactions can become an asset of 3D FFM as it provides insights into colloidal interactions in addition to producing a more systematic and self-consistent analysis of the interfacial solution structure”

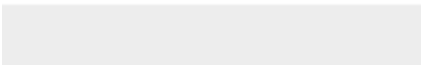



Click here to access/download
Supplemental Coding Files
ReadMe Matlab Files.txt





Click here to access/download
Supplemental Coding Files
Process_MultipleFiles_h5Data.m





Click here to access/download
Supplemental Coding Files
`Analyze_kCalculate_SaveVideos.m`

